Summer 6-24-2014

Fluid flows through unsaturated porous media: An alternative simulation procedure

Maria Laura Martins-Costa
Universidade Federal Fluminense

Joao Carlos Castro Dias
Universidade Federal Fluminense

Rogerio M. Saldanha da Gama
Universidade do Estado do Rio de Janeiro

Proceedings of the 5th International Conference on Porous Media and its Applications in Science and Engineering
ICPM5
June 22-27, 2014, Kona, Hawaii

FLUID FLOWS THROUGH UNSATURATED POROUS MEDIA: AN ALTERNATIVE SIMULATION PROCEDURE

Maria Laura Martins-Costa and João Carlos Castro Dias

Laboratory of Theoretical and Applied Mechanics, Mechanical Engineering Department, PGMEC, Universidade Federal Fluminense, 24210-240, Niterói, RJ, Brazil

Rogério M. Saldanha da Gama

Mechanical Engineering Department, Universidade do Estado do Rio de Janeiro, 20550-013, Rio de Janeiro, RJ, Brazil

ABSTRACT

This article studies fluid flows through an unsaturated porous matrix, modeled under a mixture theory viewpoint, which give rise to nonlinear hyperbolic systems. An alternative procedure is employed to simulate these nonlinear nonhomogeneous hyperbolic systems of two partial differential equations representing mass and momentum conservation for the fluid (liquid) constituent of mixture. An operator splitting technique is employed so that the nonhomogeneous system is split into a time-dependent ordinary portion and a homogeneous one. This latter is simulated by employing Glimm's scheme and an approximate Riemann solver is used for marching between two consecutive time steps. This Riemann solver conveniently approximates the solution of the associated Riemann problem by piecewise constant functions always satisfying the jump condition – giving rise to an approximation easier to implement with lower computational cost. Comparison with the standard procedure, employing the complete solution of the associated Riemann problem for implementing Glimm's scheme, has shown good agreement.

INTRODUCTION

Transport phenomena are usually described by parabolic or elliptic partial differential equations – always giving rise to regular solutions, however hyperbolic systems describe better flows through unsaturated porous media, although they may not admit a regular solution, but a generalized one, involving shock waves. Glimm's scheme is a reliable method with mathematically ensured accuracy, preserving the shock wave magnitude and position, specially developed to deal with discontinuous problems. However, besides being limited to treat one-dimensional problems, it requires the complete solution of an associated Riemann problem for marching between each two consecutive time steps.

This work employs an alternative procedure – namely an approximate Riemann solver – developed by Saldanha da Gama and Martins-Costa (2008), which circumvents the requirement of a complete solution of the associated Riemann problem. This Riemann solver approximates the solution of the associated Riemann problem by piecewise constant functions – instead of using the four possible solutions of the complete solution of the Riemann problem – giving rise to an approximation easier to implement with lower computational cost.

The mechanical model uses a Continuum Mixture Theory approach, in which the unsaturated porous medium is modeled as a mixture of three overlapping continuous constituents: a solid (a rigid, homogeneous and isotropic porous matrix), a liquid (an incompressible fluid) and an inert gas, accounting for the compressibility of the system. The mathematical model generates a nonlinear nonhomogeneous hyperbolic system of two partial differential equations.

The resulting nonlinear problem is simulated treating two simultaneous problems as if they were sequential: the operator is split into a non-homogeneous (time-dependent) ordinary part and a homogeneous hyperbolic one. This latter is simulated by a Glimm's scheme for evolution in time, employing an approximate Riemann solver proposed by Saldanha da Gama and Martins-Costa (2008) for each two consecutive steps. The employed Riemann solver approximates the solution of the associated Riemann problem by piecewise constant functions always satisfying the jump condition, but not necessarily the entropy conditions (Smoller, 1983). The above-mentioned procedure, associated with the combination of Glimm's scheme and an operator splitting technique, provides a convenient way for simulating hyperbolic systems. A comparison among results obtained by employing an exact solution of the

associated Riemann problem with the Riemann solver results shows the good performance of the latter strategy.

1 Mechanical Model

Considering a chemically non reacting mixture of a rigid solid constituent at rest, a liquid constituent – from now on denoted as fluid constituent and an inert gas, included to account for the compressibility of the mixture as a whole – it suffices to solve mass and momentum balance equations for the fluid constituent (Atkin and Craine, 1976; Rajagopal and Tao, 1995)

$$\begin{aligned} &\frac{\partial \rho_F}{\partial t} + \nabla \cdot (\rho_F \mathbf{v}_F) = 0 \\ &\rho_F \left[\frac{\partial \mathbf{v}_F}{\partial t} + (\nabla \mathbf{v}_F)\mathbf{v}_F \right] \\ &\qquad = \nabla \cdot \mathbf{T}_F + \mathbf{m}_F + \rho_F \mathbf{b}_F \end{aligned} \tag{1}$$

where ρ_F is the fluid constituent mass density (the local ratio between the fluid constituent mass and the corresponding volume of mixture), $\mathbf{v}_F$ its velocity in the mixture, $\mathbf{T}_F$ represents the partial stress tensor associated with the fluid constituent, $\mathbf{b}_F$ is the body force (per unit mass) and $\mathbf{m}_F$ is the momentum supply acting on the fluid constituent due to its interaction with the remaining constituents of the mixture.

Constitutive relations for the partial stress tensor associated with the fluid constituent ($\mathbf{T}_F = -\varphi \bar{p} \mathbf{I}$) and the momentum supply acting on the fluid constituent ($\mathbf{m}_F = -\left(\mu_f / K\right)\varphi^2 \mathbf{v}_F - \left(\mu_f D\right)/ K \nabla \varphi$) are explained in Saldanha da Gama et al. (2001). In these equations μ_f represents the fluid viscosity, K the porous matrix specific permeability (both measured considering a Continuum Mechanics viewpoint), D a diffusion coefficient (analogous to the usual mass diffusion coefficient), $\bar{p}$ is a pressure (assumed constant while the flow is unsaturated) and φ is the fluid fraction. It is important to note that the ratio between the fluid fraction φ and the porous matrix porosity ε is defined as the saturation ψ, so that $\psi = \varphi / \varepsilon = \rho_F / \rho_F^*$, with $0 < \psi \le 1$, $0 < \psi \le 1$, in which ρ_f is the actual mass density of the fluid – regarded as a single continuum, in contrast to ρ_F defined as the fluid constituent mass density. Neglecting the first term of $\mathbf{m}_F$, the Darcian term, and making $\tilde{p} = \bar{p}\varphi + \left(\mu_f D\right)/ K\varphi$, the mechanical model for an isothermal flow may be written as

$$\begin{cases} \dfrac{\partial \varphi}{\partial t} + \dfrac{\partial}{\partial r}\left(\varphi \tilde{v}\right) = -\dfrac{\varphi \tilde{v}}{r} \\ \dfrac{\partial}{\partial t}\left(\varphi \tilde{v}\right) + \dfrac{\partial}{\partial r}\left(\tilde{p} + \varphi \tilde{v}^2\right) = -\dfrac{\varphi \tilde{v}^2}{r} \\ \dfrac{\partial F}{\partial \tau} + \dfrac{\partial G}{\partial \eta} = -\dfrac{1}{\eta} G \\ \dfrac{\partial G}{\partial \tau} + \dfrac{\partial}{\partial \eta}\left(\dfrac{G^2}{F} + p\right) = -\dfrac{1}{\eta}\dfrac{G^2}{F} \end{cases} \tag{2}$$

in which $\tilde{v}$ is the is the only non-vanishing component of the fluid constituent velocity $\mathbf{v}_F$, the pressure is such that $p = c\varphi$ (c being a constant) and the system at the right side of equation (2) was obtained employing the following redefinition: $F \equiv \varphi$, $G \equiv \varphi v$ combined with the dimensionless quantities: $\eta = r / R$, $\tau = t\breve{v} / R$, $v = \tilde{v} / \breve{v}$ and $p = \tilde{p} / \varphi \breve{v}^2$, in which R is a reference radius, $\breve{v}$ a reference velocity

2 Glimm's Scheme and Operator Splitting

The first step consists in obtaining an initial approximation for (F, G) by advancing $\Delta\tau$ in time through the homogeneous part of the operator via Glimm's method, using the values of (F, G) at time $\tau=\tau_n$ as initial data. The numerical approximation for the solution at time $\tau=\tau_n$ is then obtained by advancing in time with the same time step $\Delta\tau$ through the purely time evolutionary system. This procedure is repeated until reaching a specified simulation time. The numerical procedure employed to advance from the time $\tau=\tau_n$ to $\tau=\tau_{n+1}$ may be defined as the combination of problem (2) with $F = \hat{F}_n(\eta)$; $G = \hat{G}_n(\eta)$ at $\tau = \tau_n$. First an initial approximation for (F, G,) is obtained by applying Glimm's method to the homogeneous associated system, subsequently the numerical approximation for the solution at time $\tau=\tau_{n+1}$ is finally reached by advancing in time to solve the following time evolutionary problem, with the same step $\Delta\tau=\tau_{n+1}-\tau_n$ through equations:

$$\begin{cases} \dfrac{\partial F}{\partial \tau} = -\dfrac{2}{\eta} G & F = \hat{F}_{n+1}\left(\eta\right) \\ \dfrac{\partial G}{\partial \tau} = -\dfrac{2}{\eta}\dfrac{G^2}{F} & G = \hat{G}_{n+1}\left(\eta\right) \end{cases} \text{ at } \tau = \tau_n$$

$$F = \hat{F}_{n+1}\left(\eta\right) \approx \tilde{F}_{n+1}\left(\eta\right) - \left\{\frac{2}{\eta}\tilde{G}_{n+1}\left(\eta\right)\right\}\Delta\tau \tag{3}$$

$$G = \hat{G}_{n+1}\left(\eta\right) \approx \tilde{G}_{n+1}\left(\eta\right) - \left\{\frac{2}{\eta}\frac{\left[\tilde{G}_{n+1}\left(\eta\right)\right]^2}{\tilde{F}_{n+1}\left(\eta\right)}\right\}\Delta\tau$$

in which the right hand side of equation (3) indicates the approximations obtained by an Euler Scheme.

Glimm's scheme, specifically developed to deal with discontinuous problems, preserves the shock waves magnitude and position, within an uncertainty of $\Delta\eta$ (width of each step), however it is limited to one-dimensional problems. In order to obtain the numerical approximation for the fields F and G at τ_{n+1} – denoted as $\bar{F}_{n+1}$ and $\bar{G}_{n+1}$, the solution (or approximation) of the Riemann problem associated with the homogeneous portion of equation (2) must be known. Essentially Glimm's scheme consists in performing time evolutions by solving the associated Riemann problem between each two consecutive steps. In short, Glimm's method builds a solution for initial value problems – nonlinear hyperbolic systems subjected to arbitrary initial data – through the solution (or approximation) of as many Riemann problems as desired, to march from time $\tau=\tau_n$ to time τ_{n+1}. Initially, the initial condition – given by a function of the position η – is approximated by piecewise constant functions. In the sequence, a Riemann problem, an initial value problem whose initial condition must be a step function, is to be solved – either exactly or by employing a Riemann solver – for each two consecutive steps (Martins-Costa and Saldanha da Gama, 2001; Saldanha da Gama and Martins-Costa, 2008). The fields $\tilde{F}_{n+1}(\eta)$ and $\tilde{G}_{n+1}(\eta)$ used as initial data in the time evolutionary problem (3) are obtained by advancing $\Delta\tau$ in time employing Glimm's method to approximate the following homogeneous problem:

$$\begin{cases} \dfrac{\partial F}{\partial \tau}+\dfrac{\partial G}{\partial \eta}=0 \\ \dfrac{\partial G}{\partial \tau}+\dfrac{\partial}{\partial \eta}\left(\dfrac{G^2}{F}+p\right)=0 \\ F=\hat{F}_n(\eta) \\ G=\hat{G}_n(\eta) \end{cases} \quad \text{at } \tau=\tau_n \tag{4}$$

The generalized solution of the Riemann problem associated with the hyperbolic system (4), is reached by connecting the left (L) and right (R) states – using an intermediate constant state (*) – either by rarefactions or shocks.

System (4) is approximated by employing Glimm's scheme (Martins-Costa and Saldanha da Gama, 2001), to advance from time t_n to time t_{n+1}, in other words, $\tilde{F}_{n+1}(\eta)$ and $\tilde{G}_{n+1}(\eta)$ are the solutions of (4) evaluated at the time $\tau=\tau_{n+1}$. The strategy for building a solution for an initial value problem consists of appropriately gathering the solution of a certain previously chosen number of Riemann problems to successively march from time $\tau=\tau_n$ to time $\tau_{n+1}=\tau_n+\Delta\tau$. The arbitrary initial condition given by a function of the position η ($F(\eta,0)=F_0(\eta)$, $G(\eta,0)=G_0(\eta)$) is approximated by piecewise constant functions, by convenience, with equal width steps:

$$\begin{aligned} F&=\hat{F}_n(\eta)\approx F_{n_j}=\hat{F}_n\left(\eta_j+\theta_n\Delta\eta\right) \\ G&=\hat{G}_n(\eta)\approx G_{n_j}=\hat{G}_n\left(\eta_j+\theta_n\Delta\eta\right) \\ &\text{for}\quad \eta_j-\frac{\Delta\eta}{2}<\eta<\eta_j+\frac{\Delta\eta}{2} \end{aligned} \tag{5}$$

in which θ_n is a number randomly chosen in the open interval $(-1/2\ ,+1/2)$ and $\Delta\eta$ is the width of each step ($\Delta\eta=\eta_{j+1}-\eta_j$).

The approximations for the initial data at a given time τ_j presented in equation (6) give rise, for each two consecutive steps, to the following Riemann problem:

$$\begin{cases} \dfrac{\partial F}{\partial \tau}+\dfrac{\partial G}{\partial \eta}=0 \\ \dfrac{\partial G}{\partial \tau}+\dfrac{\partial}{\partial \eta}\left(\dfrac{G^2}{F}+p(F)\right)=0 \\ (F,G)=\left(F_{n_j},G_{n_j}\right) \quad \tau=\tau_n\ ,-\infty<\eta<\eta_j+\dfrac{\Delta\eta}{2} \\ (F,G)=\left(F_{n_{j+1}},G_{n_{j+1}}\right) \quad \tau=\tau_n\ ,\ \eta_{j+1}-\dfrac{\Delta\eta}{2}<\eta<\infty \end{cases} \tag{6}$$

Denoting by $\bar{F}_{n_j}$ and $\bar{G}_{n_j}$ the generalized solution of the Riemann problem (6), the approximation for the solution of (4) at the time $\tau=\tau_{n+1}$ is given by: $F=\hat{F}_{n+1}(\eta)\approx\bar{F}_{n_j}(\eta,\tau_{n+1})$ and $G=\hat{G}_{n+1}(\eta)\approx\bar{G}_{n_j}(\eta,\tau_{n+1})$, for $\eta_j<\eta<\eta_{j+1}$.

It is important to note that in order to prevent interactions among nearby waves of adjacent Riemann problems, the time step Δt must be chosen in such a way that the Courant-Friedrichs-Lewy (CFL) condition (Smoller, 1983) is satisfied, thus assuring uniqueness for the solution: $t_{n+1}-t_n\le\Delta x/\left(2\left|\lambda\right|_{\max}\right)$, with $\left|\lambda\right|_{\max}$ representing the maximum (in absolute value) propagation speed of shocks, considering all the Riemann problems at time t_n.

At this point it is important to stress some features of Glimm's method. First if the width of the steps tends to zero the approximation obtained by Glimm's method tends to the exact solution of the problem considering its weak formulation. Another characteristic of Glimm's

scheme is that it preserves shock magnitude (no diffusion being observed) and position – whose admissible deviation from the correct position is of the order of magnitude of the width of each step Δx for each time advance.

3 The Riemann Solver

The approximate Riemann solver employed (Saldanha da Gama and Martins-Costa, 2008) consists of assuming the solution for system (6) within a space of piecewise constant functions, so that any two states are be connected by a discontinuity. In other words: $(F_L,G_L) \rightarrow$ 1-shock $\rightarrow (F_*,G_*) \rightarrow$ 2-shock $\rightarrow (F_R,G_R)$.

This approximation no longer requires considering the original four possible solutions, connected either by rarefactions or by shocks: $\left(F_L,G_L\right) \underset{Raref \text{ or } Shock}{\Longrightarrow} \left(F_*,G_*\right) \underset{Raref \text{ or } Shock}{\Longrightarrow} \left(F_R,G_R\right)$. On the other hand, the entropy conditions are not ensured. It is to be noted that the conservation laws are satisfied in a weak sense.

The (generalized) solution of equation (6), within a space of piecewise constant functions, is reached as follows

$$\left(F,G\right)=\begin{cases}\left(F_L,G_L\right) & \text{if } -\infty<(\eta-\overline{\eta})/(\tau-\overline{\tau})<s_1\\ \left(F_*,G_*\right) & \text{if } s_1<(\eta-\overline{\eta})/(\tau-\overline{\tau})<s_2\\ \left(F_R,G_R\right) & \text{if } s_2<(\eta-\overline{\eta})/(\tau-\overline{\tau})<\infty\end{cases} \quad (7)$$

4 Numerical Results

Figures 1 to 3 show a comparison employing the alternative procedure (Riemann solver) and the standard one (Riemann problem exact solution), for distinct initial-value problems. In all cases the evolution for fluid fraction and dimensionless velocity variation with radial position for a cylindrical wellbore the cylinder's internal radius is depicted at the left-hand side while the external one is at the right side; considering six selected time instants, the first one representing the initial condition. In all the depicted results the vertical axis corresponds to the numerical value assumed by fluid fraction and velocity, while the horizontal one represents the spatial coordinate η. In all cases, distinct internal radii are used: in case (a) R_i=0.05 while in case (b) R_i=2.05, to evaluate the influence of the radius of curvature.

The two columns at the left-hand side – namely a set composed by two columns and six lines, each line representing a distinct time instant – depict fluid fraction and velocity obtained by employing Glimm's scheme with 300 steps for each time advance built from the exact solution of the associated Riemann problem. The two columns at the right-hand side show equivalent results for fluid fraction and velocity also obtained by using Glimm's scheme with 300 steps for each advance in time but constructed by using the Riemann solver used in this work. In all the depicted problems it is important to note the good performance of the Riemann solver.

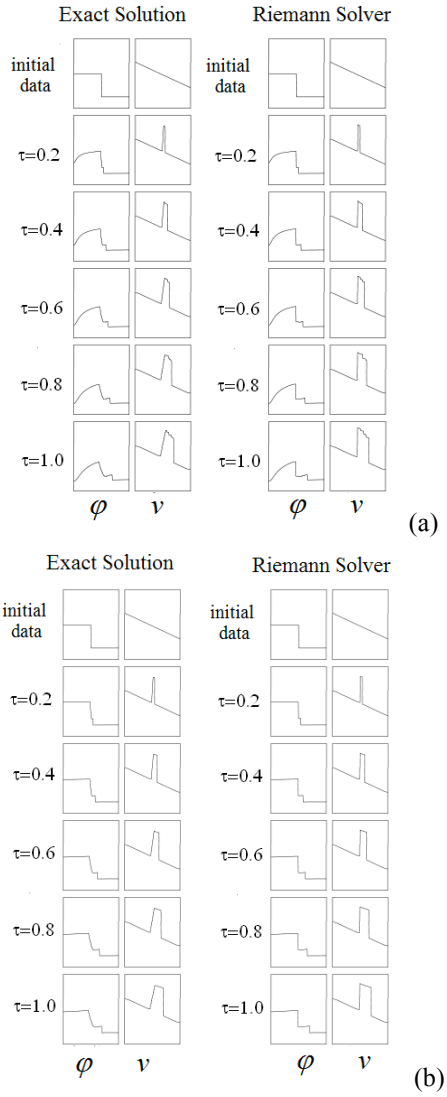

Figure 1: Fluid fraction and dimensionless velocity variation with radial position for a cylindrical wellbore; initial data: linear decreasing velocity and step function fluid fraction.

Figures 1 to 3 show a comparison employing the alternative procedure (Riemann solver) and the standard one (Riemann problem exact solution), for distinct initial-value problems. In all cases the evolution for fluid fraction and dimensionless velocity variation with radial position for a cylindrical wellbore the cylinder's internal radius is depicted at the left-hand side while the external one is at the right side; considering six selected time instants, the first one representing the initial condition. In all the depicted results the vertical axis corresponds to the numerical value assumed by fluid fraction and velocity, while the horizontal one represents the spatial coordinate η. In all cases, distinct internal radii are used:

in case (a) R_i=0.05 while in case (b) R_i=2.05, to evaluate the influence of the radius of curvature.

The two columns at the left-hand side – namely a set composed by two columns and six lines, each line representing a distinct time instant – depict fluid fraction and velocity obtained by employing Glimm's scheme with 300 steps for each time advance built from the exact solution of the associated Riemann problem. The two columns at the right-hand side show equivalent results for fluid fraction and velocity also obtained by using Glimm's scheme with 300 steps for each advance in time but constructed by using the Riemann solver used in this work. In all the depicted problems it is important to note the good performance of the Riemann solver.

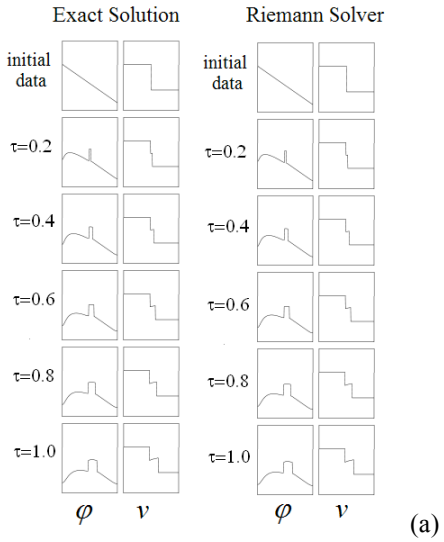

Figure 2. Fluid fraction and dimensionless velocity variation with radial position for a cylindrical wellbore initial data: linear decreasing fluid fraction and step function velocity.

Figure 1 presents results for initial data given by a linear decreasing velocity ($v_0 = (N - I + 1.)/N$) and step function fluid fraction ($\varphi_{0_L} = 0.7$, $\varphi_{0_R} = 0.1$). It shows a very good agreement when comparing the left and the right sides, with the velocity evolution showing some minor differences – namely when a connection by rarefaction was used to obtain the exact solution. Comparing figures 1a (R_i=0.05) and 1b (R_i=2.05) it may be noted the influence of the radius of curvature, as R_i increases the curvature of the fluid fraction near the internal cylindrical shell radius decreases, while the velocity presents a more uniform behavior in the jump.

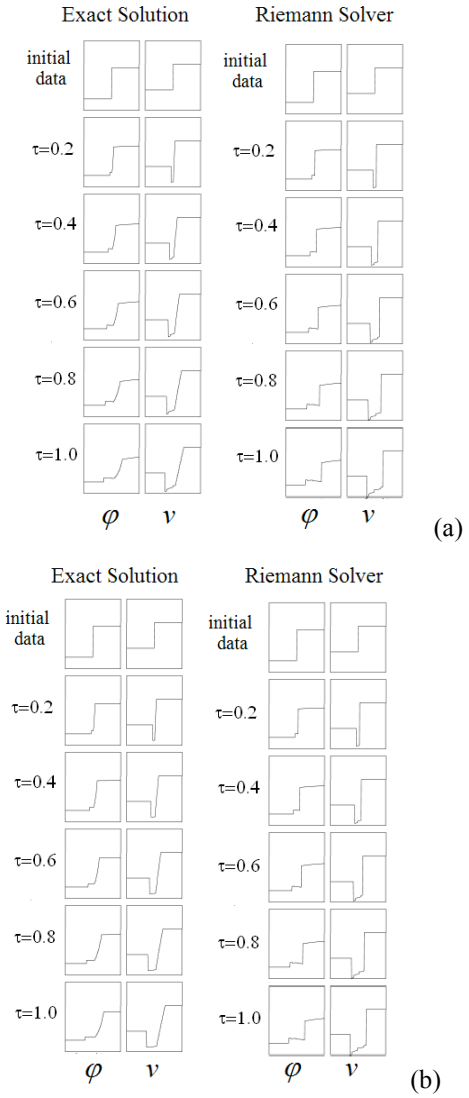

Figure 3. Fluid fraction and dimensionless velocity variation with radial position for a cylindrical wellbore initial data: step function velocity and fluid fraction.

In Figure 2 the initial data consist of a shock prescribed for the velocity – a step function with

($v_{0_L} = 1.0,\ v_{0_R} = 0.0$) while the fluid fraction is given by a linear decreasing function ($\varphi_0 = (N - I + 1.)/N$).

Since the results obtained through the exact solution of Riemann problem, depicted at the first two columns, give rise essentially to connections by shocks, the Riemann solver employed in this work (depicted at the two last columns) shows a very good agreement with those obtained by employing the exact solution. Comparing figures 2a (R_i=0.05) and 2b (R_i=2.05) for verifying the influence of the radius of curvature it may be noted again that as the internal cylindrical shell radius increases the curvature of the fluid fraction near the internal cylinder radius decreases, while the influence on the velocity behavior is barely noticeable.

In Figure 3 the initial data is given by two distinct (increasing) step functions for the velocity ($v_{0_L} = 0.0,\ v_{0_R} = 1.0$) and the fluid fraction ($\varphi_{0_L} = 0.1,\ \varphi_{0_R} = 0.9$). Like in the case considered in Figure 2, the results obtained employing the exact solution of Riemann problem give rise to connections by shocks, so they present very good agreement with those obtained with Riemann solver. The influence of the radius of curvature is observed by comparing figures 3a (R_i=0.05) and 3b (R_i=2.05). As the internal cylindrical shell radius increases the curvature of the fluid fraction near the external cylindrical shell radius decreases (opposing the behavior verified in Figures 1 and 2), while, like in Figure 2, there is almost no influence on the velocity behavior.

CONCLUSIONS

The numerical methodology presented in this work allowed the accurate approximation of a nonlinear nonhomogeneous hyperbolic system of partial differential equations, simulated by combining Glimm's scheme and an operator splitting technique. This operator splitting procedure (in which the homogeneous part of the operator is split away from the purely time evolutionary one) has shown a good performance when the homogeneous associated problem simulation employed an approximate Riemann solver (Saldanha da Gama and Martins-Costa, 2008). This Riemann solver was employed to implement Glimm's method for advancing in time. Glimm's scheme was also implemented using the complete solution of the associated Riemann problem and comparison of qualitative results employing these two methodologies has shown very good agreement.

ACKNOWLEDGEMENT

The authors M.L. Martins-Costa and R.M. Saldanha da Gama gratefully acknowledge the financial support provided by the Brazilian agency CNPq.

REFERENCES

[1] Atkin, R.J. and Craine, R.E., 1976, "Continuum theories of mixtures. Basic theory and historical development", Quart. J. Mech. Appl. Math. Vol. 29, pp. 209-244.

[2] Martins-Costa, M.L. and Saldanha da Gama, R.M., 2001, "Numerical simulations of one-dimensional flows through porous media with shock waves", Int. J. Numerical Meth. Engng. Vol. 52, pp. 1047-1067.

[3] Rajagopal, K.R. and Tao, L., 1995, Mechanics of Mixtures, Series Advances in Math. Appl. Sci. Vol. 35, World Scientific, Singapore.

[4] Saldanha da Gama, R.M. and Martins-Costa, M.L., 2008, "An alternative procedure for approximating hyperbolic systems of conservation laws". Nonlinear Anal.: Real ,World Appl. Vol. 9, pp. 1310-1322.

[5] Smoller, J., 1983, Shock-Waves and Reaction Diffusion Equations, Springer-Verlag, Berlin.